Kafkas Universitesi Veteriner Fakultesi Dergisi
Journal Home-Page: http://vetdergikafkas.org
E-ISSN: 1309-2251

Kafkas Univ Vet Fak Derg
31 (2): 171-180, 2025
DOI: 10.9775/kvfd.2024.32852

RESEARCH ARTICLE

Stanniocalcin-1 Regulates Ca^{2+}/Pi Uptake in Bovine Renal Tubule Epithelial Cells by Modulating Expression of Entry Channels *In vitro*

Shimeng CUI [1,†] Xueying YI [1,†] Xiaoliang XIANG [1,2] Yaxin TANG [1] Xuewei PENG [1] Xuefeng WANG [1] Quan YANG [1] Kejia ZHANG [1] Liming WU [1,2 (*)]

† *These authors contributed equally to this study*

[1] College of Biological and Food Engineering, Huaihua University, Huaihua 418008, CHINA
[2] Key Laboratory of Research and Utilization of Ethnomedicinal Plant Resources of Hunan Province, Huaihua University, Huaihua 418008, CHINA

(*) **Corresponding author:**
Liming WU
Phone: +86 13687380828
E-mail: wlm@hhtc.edu.cn

How to cite this article?
Cui S, Yi X, Xiang X, Tang Y, Peng X, Wang X, Yang Q, Zhang K, Wu L: Stanniocalcin-1 regulates Ca^{2+}/Pi uptake in bovine renal tubule epithelial cells by modulating expression of entry channels *in vitro*. *Kafkas Univ Vet Fak Derg*, 31 (2): 171-180, 2025.
DOI: 10.9775/kvfd.2024.32852

Article ID: KVFD-2024-32852
Received: 22.08.2024
Accepted: 22.01.2025
Published Online: 18.03.2025

Abstract

Stanniocalcin-1 (STC1), a glycoprotein, serves as an autocrine or paracrine factor in multiple processes in mammals, including the regulation of calcium/phosphorus (Ca^{2+}/Pi) transport. However, its underlying mechanisms are not fully elucidated. Here, we examined the intracellular Ca^{2+} ($[Ca^{2+}]_i$) and Pi concentrations ($[Pi]_i$) levels in primary bovine renal tubular epithelial cells (RTECs) using flow cytometry and phosphomolybdic spectrophotometry, respectively, following STC1 overexpression/inhibition, and treatments with vitamin D_3 receptor (VDR) agonist calcitriol or antagonist MeTC7. The expression of Ca^{2+}/Pi transporters (TRPV5, TRPV6, CB-D_{28K}, PMCA1b, NCX1, Npt2a, Npt2c) was measured by real-time qPCR and western blotting. The results revealed STC1 inhibition by STC1-shRNA promoted Ca^{2+} intake and inhibited Pi influx, whereas STC1 overexpression by pcDNA3.1/STC1 had the opposite effects. The calcitriol-induced increase in $[Ca^{2+}]_i$ was reversed by STC1 overexpression and MeTC7 treatment. Overexpression of STC1 reduced the expression of TRPV5, TRPV6, and VDR, while suppressing calcitriol-induced TRPV5 upregulation and enhancing Npt2a/Npt2c expression. STC1 had no effect on CB-D_{28K}, NCX1, or PMCA1b, which mediate Ca^{2+} diffusion and extrusion. In conclusion, our findings suggest STC1 inhibits Ca^{2+} transport and enhances Pi uptake in RTECs at least partly by regulating TRPV5/TRPV6 and Npt2a/Npt2c expression, respectively. Interference of 1,25 $(OH)_2D_3$/VDR axis may also contribute. The present findings provide new insights into the underlying mechanisms of STC1 and offer strategies to prevent mineral disorders in cattle.

Keywords: Ca^{2+}/Pi transport, TRPV5/6, Npt2a/2c, RTECs, Stanniocalcin-1

INTRODUCTION

Calcium (Ca^{2+}) and phosphorus (inorganic phosphate, Pi) are essential macrominerals that collaborate in various physiological processes, including bone formation, metabolic regulation, and milk production. Imbalances in Ca^{2+}/Pi levels in cattle, especially in the perinatal and lactating cows, can lead to severe metabolic disorders such as rickets, osteomalacia, and milk fever, which not only affect animal health but also result in substantial economic losses in the dairy and meat industries.Their balance is maintained through the coordinated actions of the gastrointestinal tract, bones, and kidneys. The kidneys play a key role by excreting an amount of Ca^{2+}/Pi equal to what is absorbed by gut, a process achieved via glomerular filtration and reabsorption in the renal tubules.

In mammals, reabsorption of Ca^{2+} by the renal tubules involves two distinct mechanisms: paracellular and transcellular pathways. Paracellular transport is a passive, non-saturated, and poorly regulated process. In contrast, active transcellular transport is a saturable and finely orchestrated process [1] comprising three steps. First, Ca^{2+} entry via epithelial Ca^{2+} channels in the apical membrane, such as transient receptor potential vanilloid receptor subtype 5 and 6 (TRPV5 and TRPV6) [2]. Second, Ca^{2+} binds to calbindin-D_{28k} (CB-D_{28k}), facilitating intracellular diffusion [3]. Third, Ca^{2+} efflux by the coordinated action of plasma membrane Ca^{2+} ATPase 1b (PMCA1b) and Na^+/Ca^{2+} exchanger 1 (NCX1) at the basolateral membrane [4]. 1,25-dihydroxyvitamin D_3 (1,25$(OH)_2D_3$, calcitriol) and its nuclear receptor, vitamin D_3 receptor (VDR), play

a central role in regulating the entire process of Ca^{2+} transport and regulation.

The renal absorption of Pi also occurs via two pathways: an active, transcellular sodium-dependent and a passive, paracellular pathway. Sodium-dependent phosphate co-transporter 2a and 2c (Npt2a and Npt2c) are exclusively expressed on the apical membrane of proximal RTECs and are responsible for transcellular Pi transport [5]. However, the mechanism by which Pi is extruded at the basolateral membrane of RTECs remains unclear.

Systemic Ca^{2+}/Pi homeostasis is mainly maintained through crosstalk among cells of the gastrointestinal tract, bone, kidney, and parathyroid gland. The coordinated action of transport proteins and regulatory factors, such as $1,25(OH)_2D_3$, parathyroid hormone, calcitonin [6], fibroblast growth factor 23, and αKlotho [7], constitute the key molecular mechanisms that ensure the maintenance of this homeostasis.

In addition to the aforementioned hormones and cytokines, STC1 appears to be another key player in this intricate regulatory network contributing to Ca^{2+}/Pi homeostasis in mammals, just similar to the function of its homolog (STC) in fish. Beyond its function in mineral homeostasis regulation, STC1 exhibits a wide range of effects, including promoting cell proliferation [8], anti-inflammatory and anti-oxidative activities [9-11], and mitigating nerve damage [12]. Furthermore, STC1 is expressed in almost all tissues [13, 14] but is typically absent from the circulation, suggesting that it may function as a paracrine/autocrine factor rather than as a classical endocrine hormone [15].

Although STC1 is expressed in multiple tissues and organs across various species and is involved in diverse biological and pathological processes, its regulatory effects on Ca^{2+}/Pi homeostasis are conserved. However, the precise molecular mechanism through which STC1 affects renal Ca^{2+}/Pi transport has not been thoroughly elucidated. This study will utilize a primary bovine renal tubule epithelial cell model, as these cells exhibit closer physiological similarities to the renal tubule of normal cattle, to provide more precise insights into the role of STC1 in the active transport of Ca^{2+}/Pi at cellular level, as well as its potential molecular mechanisms responsible for regulating bovine mineral metabolism.

Material and Methods

Ethical Statement

The experimental protocol was approved by the official Committee on the Ethics of Animal Experiments of Huaihua University [Approval no: 2024 (A01006)].

Primary Culture of Bovine RTECs

Primary bovine RTECs were isolated from the kidney cortex of the 1-day-old Chinese Holstein calves. The calves were humanely euthanized under anesthesia using an electric shock apparatus (Jianhua Co., Ltd, Qingdao, China). The kidney cortices were aseptically removed, dissected and minced into small pieces in pre-cooled D-Hank's buffer. The tissue was then ground using a 100-mesh steel wire sieve and filtered through a 150-mesh sieve. The retained cell clusters were collected and evenly dispersed by pipetting. After two rounds of centrifugation at 1200 rpm for 5 min each, the pellets were resuspended in 1 mL of 1 mg/mL collagenase I (Sigma, St. Louis, USA) and incubated at 37°C for 20 min with shaking. An equal volume of DMEM/F12 containing 10% FBS (Gibco, Carlsbad, USA) was then added to neutralize the enzyme. Following another round of centrifugation at 1200 rpm for 5 min, the pellet was resuspended in DMEM/F12 supplemented with 10% FBS, 100 U/mL penicillin, and 100 mg/L streptomycin and incubated at 37°C in a 5% CO_2 atmosphere until confluent. Immunocytochemistry staining was performed using mouse anti-PCK (Pan Cytokeratin, #BM0034, Boster, Wuhan, China), CK18 (Cytokeratin 18, BM4594, Boster), and vimentin monoclonal antibodies (BM0135, Boster) to distinguish epithelial cells from other cell types in the culture, as previously described [10]. The MDBK (Madin-Darby Bovine Kidney) cell line (GDC0290, CCTCC, Wuhan) served as a positive control.

Construction of STC-1 Expression Vector

Total RNA was extracted from calf kidney using Trizol reagent (Invitrogen, Carlsbad, USA) and converted to cDNA by a cDNA Synthesis Kit (TaKaRa, Dalian, China). Bovine full-CDS sequences of *STC1* were amplified using the primers listed in *Table 1*. The purified amplicons were digested with restriction enzymes *BamHI* and *XhoI* (TaKaRa) and ligated into the pcDNA3.1(+) expression vector (Invitrogen) using T4 DNA ligase (TaKaRa). The resulting recombinant plasmid, confirmed by DNA sequencing, was designated as pcDNA3.1/STC1. The extraction of endotoxin-free plasmid DNA from an overnight culture of *E. coli* DH5α (Invitrogen) harboring pcDNA3.1/STC1 was performed using a commercial kit (D6926-03, Omega, Doraville, USA).

Design of Annealed Oligonucleotides of Small Hairpin RNA (shRNA)

The shRNA oligonucleotide duplexes targeting bovine STC1 were designed online (Invitrogen Block-iT RNAi Designer) and synthesized by Huayu Gene Co., Ltd (Wuhan, China), the sequences were as follows: 5′-ccgg *ggatgtacgacatctgtaaat* ctcgag *atttacagatgtcgtacatcc* ttttg-3′ (Forward oligo) and 5′-aattcaaaaa *ggatgtacgacatctgtaaat* ctcgag *atttacagatgtcgtacatcc*-3′ (Reverse oligo). A functional non-targeted shRNA sequence (Addgene plasmid#1864, a gift from David Sabatini Lab) used as the negative control.

Table 1. *The primer sequences used in this study for gene clone and real-time qPCR analysis*

Gene	Genebank Accession No.	Primer (5'-3')	Product Length (bp)	Annealing Temperature (°C)
STC1 (for gene clone)	NM_176669.3	**GGATCC**CTCAGAGAATGCTCCAAAACTCA	744	60°C
		CTCGAGCTCCCCAGCTAGGCACT		
STC1(for qPCR)	NM_176669.3	GCTTCTGGTGCTGGTGAT	211	56°C
		GAAGGATTTACAGATGTCGTAC		
TRPV5	XM_010804626.3	GATTCGCCTCAGCGTTCT	148	56°C
		GGCAAGTCCACATCGTAGTT		
TRPV6	NM_001206189.1	CAATGAAACTGACCCCCG	195	56°C
		CCGAGTATGGTCTGTCCGA		
Npt2a	NM_001103223.1	AACGCCATCCTGTCCAAT	122	56°C
		AGAAGAGACCATGCTGACC		
Npt2c	XM_024999684.1	GTCATCAACGCCGACTTC	272	57°C
		AAGTGGATGAGAGCGACCT		
VDR	NM_001167932.2	ACAGTGAGGACGAGGGGAA	110	59°C
		CATTGTGTCTGGAGAGGAGGT		
NCX1	NM_176632.2	CTTAGATGGAGCCCTGGTT	191	56°C
		GAATACGGTAAAACGCTCG		
PMCA1	NM_174696.2	ATAGAACAGTGGCTATGGTCAA	152	56°C
		TCCGCTAACTCCTCCTCG		
CB-D_{28k}	NM_001076195.1	ACGGAAGTGGTTACCTGGA	88	56°C
		GATAACTCCAAACCAGCCTT		
GAPDH	NM_001034034.2	CACTCACTCTTCTACCTTCG	109	56°C
		CACCACCCTGTTGCTGT		

STC1, stanniocalcin-1; TRPV5 and 6, transient receptor potential vanilloid receptor subtype 5 and 6; Npt2a, sodium-dependent phosphate co-transporter 2b; Npt2c, sodium-dependent phosphate co-transporter 2c; VDR, vitamin D receptor; NCX1, sodium/calcium exchanger 1; PMCA1, plasma membraneCa^{2+}-ATPase 1; CB-D_{28k}, calbindin-D_{28K}; GAPDH, glyceraldehyde-3-phosphate dehydrogenase

The yielded double-stranded oligonucleotides were cloned into pLVX-Puro vector (TaKaRa) between the *Eco*RI and *Age*I (TaKaRa) restriction sites. The recombinant vectors designated STC1-shRNA and scrambled shRNA after sequencing, respectively.

Transfection and Treatment of RTECs

RTECs were detached using 0.25% trypsin (Gibco), and then seeded in a 6-well plate at a density of 2 x 10^5 cells/well. Cells were incubated in growth medium until 60%-70% confluence. After rinsing thoroughly with sterile PBS, lipofectamine™ 3000 (Invitrogen) was employed to transfect the cell with pcDNA3.1/STC1 (2.5 μg/well) or an equivalent amount of pcDNA3.1(+), STC1-shRNA, scrambled shRNA, or pLVX-puro plasmids. After a 48-h incubation in growth medium, total RNA, protein, and cells were harvested for further analysis.

To investigate whether STC1 regulates Ca^{2+} absorption through the 1,25$(OH)_2D_3$/VDR axis, approximately 2 x 10^5 RTECs were seeded in 60 mm plates, cultured in DMEM/F12 supplemented with 10% FBS, and treated with either vehicle (0.1% ethanol) or 200 nM calcitriol (HY-10002, MedChemExpress, Monmouth Junction,

Table 2. *The details of antibodies used in this study for western blotting*

Antibody Name	Host	Manufacturer	Art. No.	Dilution Ratio	Theoretical MW
STC1	Rabbit	Novus Biologicals, Littleton, USA	NBP1-59310	1:1,000	~28 kDa
TRPV5	Rabbit	Bioss, Beijing, China	bs-8534R	1:600	~90 kD
TRPV6	Rabbit	Bioss	bs-15506R	1:600	~67 kD
Npt2a	Rabbit	Novus Biologicals	NBP2-85748	1:1,000	~69 kD
Npt2c	Rabbit	Bioss	bs-20801	1:400	~63 kD
VDR	Rabbit	ABclonal, Woburn, USA	A2194	1:1,000	~60 kD
NCX1	Rabbit	Bioss	bs-1550R	1:400	~106 kD
PMCA1b	Rabbit	Bioss	bs-4978R	1:600	~138 kD
CB-D_{28k}	Rabbit	Bioss	bs-3758R	1:600	~29 kD
GAPDH	Rabbit	Bioswamp, Wuhan, China	AB36269	1:5.000	~36 kD
Anti-rabbit IgG-HRP	Goat	Servicebio, Wuhan	SAB43714	1:10.000	

STC1, stanniocalcin-1; TRPV5 and 6, transient receptor potential vanilloid receptor subtype 5 and 6; Npt2a, sodium-dependent phosphate co-transporter 2b; Npt2c, sodium-dependent phosphate co-transporter 2c; VDR, vitamin D_3 receptor; NCX1, sodium/calcium exchanger 1; PMCA1, plasma membrane Ca^{2+}-ATPase 1; CB-D_{28k}, calbindin-D_{28K}; GAPDH, glyceraldehyde-3-phosphate dehydrogenase

USA) for 48 h. The cells were then transfected with 4 µg pcDNA3.1(+) or pcDNA3.1/STC1, followed by incubation in growth medium containing 0.1% ethanol or 200 nM calcitriol for an additional 48 h. Two additional groups of cells were treated with 250 nM MeTC7 solubilized in dimethylsulfoxide for 12 h following a 48-h exposure to either 0.1% ethanol or 200 nM calcitriol [16, 17]. A separate group of cells was treated with 200 nM calcitriol alone for 60 h as a positive control. Subsequently, cells and proteins were harvested for further experiments.

Measurement of Intracellular Ca^{2+} Concentration

RTECs from each group were detached and collected by centrifugation. After three washes with PBS, cells were resuspended with 0.5 µM Fluo-3/AM (S1056, Beyotime, Shanghai, China) in PBS at 37°C for 30 min. Following two additional washes with PBS, the cells were then incubated in PBS at 37°C for 20 min. And then, the number of cells with fluorescence intensity above the baseline (positive cells) was measured using the NovoCyte™ flow cytometer (ACEA Bio, San Diego, USA) with a 1-min recording. NovoExpress software (ACEA) was used to collect and calculate the original data.

Measurement of Intracellular Pi Concentration

After treatments, about 5×10^6 cells from each group were detached and centrifuged at 1.200 × *g* for 5 min. The resulting pellets (20 µL of packed cells) were resuspended in 180 µL ddH_2O (about 10% cytocrit) and sonicated for 30 sec with 50% pulses. Following a 15-min centrifugation at 14.000 × *g*, the supernatants were collected and their Pi contents were measured using a phosphomolybdic acid kit (C006-1-1, Jiancheng, Nanjing, China). Briefly, 0.1 mL supernatant from the previous step was mixed with 0.4 mL of precipitant included in the kit, then spun at 2.200 x *g* for 10 min and the supernatant was sampled for testing. A 0.5 mM phosphorus served as standard solution. Then, 0.2 mL of sample, standard solution, and ddH_2O (blank control) were added to different test tubes. Afterward, 2 mL of a reagent mixture containing ammonium molybdate, antimony potassium tartrate, and ascorbic acid was added to each tube. Optical density (OD) values were measured at 660 nm and normalized using ddH_2O. The phosphate concentration in each tube was calculated using the formula:

$$\text{Phosphate concentration (mM)} = \frac{\text{OD(Test sample)} - \text{OD(Blank control)}}{\text{OD(Standard solution)} - \text{OD(Blank control)}} \times 0.5\ \text{mM} \times 5.$$

Real-time qPCR

The real-time qPCR reactions were performed on the CFX96 qPCR system (Bio-Rad, Hercules, USA), each reaction containing 1.0 µL cDNA, 10 µL SYBR Green qPCR Mix (KK4600, Kapa Biosystems, Wilmington, USA), 0.2 µM forward and reverse primers (Huayu gene) for each gene (*Table 1*), and DNase/RNase-free H_2O to reach a final volume of 20 µL. After a 5-min pre-denaturation at 94°C, the reactions proceeded with 40 cycles of amplification. Each cycle consists of a 5-sec denaturation at 94°C, a 10-sec annealing at 56°C-59°C (*Table 1*), and a 25-sec elongation at 72°C. A final extension step was performed at 72°C for 5 min. The data were normalized to that of *GAPDH* (data not shown).

Western Blotting

The ice-cold lysis buffer (P0013B, Beyotime) was used to prepare cell lysates. After centrifugation at 14.000 x *g* for 15 min, the supernatants were collected and standardized to 20 µg of protein per sample, then subjected to electrophoresis on a 12% SDS/PAGE gel. The separated proteins were transferred to PVDF membrane (Millipore, Bedford, USA). Following a 1-h blocking with

5% (w/v) non-fat milk, the membranes were incubated overnight with diluted rabbit polyclonal antibodies (as listed in *Table 2*). Immunoreactive bands were visualized by enhanced chemiluminescence substrate. Western blot band intensities were quantified with densitometry using an automatic analyzer (Tanon-5200, Shanghai, China).

Statistical Analysis

Data from triplicate or quadruplicate samples were subjected to one-way ANOVA using GraphPad Prism 9 software (San Diego, USA). All parameter values are expressed as the mean ± SEM. Statistical significance was defined as a P value <0.05.

Result

Microscopic Observations of Primary Cell Culture and Expression of STC1 in Transfected RTECs

After a 24-h incubation, microscopic observation showed digestion with collagenase I for 20 min with shaking yielded higher quality organoids and releasing abundant individual cells with a cobblestone-like morphology from disaggregated tubular fragments *(Fig. 1-A)*. Following a series of purification steps, the cells evenly dispersed on the T25 flasks, displaying polygonal or cuboidal shapes with distinct borders *(Fig. 1-B)*, and either dome-like or flattened appearances under phase-contrast microscopy *(Fig. 1-C)*. The morphological characteristics of the primary cultures closely resembled those of MDBK cells, which are typical epithelial cells *(Fig. 1-D)*. Moreover, both the primary cultures and MDBK cells exhibited obvious immunoreactivity for PCK *(Fig. 1-E2,F2)* and CK18 *(Fig. 1-E3,F3)* but not for vimentin *(Fig. 2-E4,F4)* or PBS *(Fig. 2-E1,F1)*, suggesting that the primary cultures predominantly consist of RTECs.

As *Fig. 1-G* shows the pcDNA3.1/STC1 plasmid significantly increased STC1 mRNA expression over 90-fold (***P<0.001) compared to control (normal cells grown in the same medium containing an equivalent volume of lipofectamine reagent) and empty vector groups, while STC1-shRNA effectively inhibited it (*P=0.0498 vs control), with no significant changes in the empty vector or scrambled shRNA groups (P>0.05). The western blotting *(Fig. 1-H,I)* further confirmed the successful up- and down-regulation of STC1 expression by pcDNA3.1/STC1 and STC1-shRNA, respectively.

Changes in the Intracellular Free Ca^{2+}/Pi Concentrations

As shown in *Fig. 2-A* and *2-B*, low STC1 expression group induced by STC1-shRNA transfection possessed higher levels of positive cells (*P=0.0189 vs control, *P=0.0123 vs scrambled shRNA group), while cells with high expression of STC1 via pcDNA3.1/STC1 transfection exhibited about half the positive signals compared to those observed in the control group (*P=0.0338) and the pcDNA3.1(+) transfection group (*P=0.0160), suggesting downregulation of STC1 expression augments cellular absorption of Ca^{2+}, while upregulation inhibits it.

In addition, cells with low STC1 expression had a lower Pi concentration in the diluted intracellular fluid (***P<0.001, ~ 2.11 mM) compared to the control and scrambled shRNA transfection groups (2.51 mM and 2.57 mM, respectively). In contrast, STC1 overexpression led to a higher Pi concentration in the cells (***P<0.001, ~ 3.51 mM). A relatively higher Pi concentration in the diluted

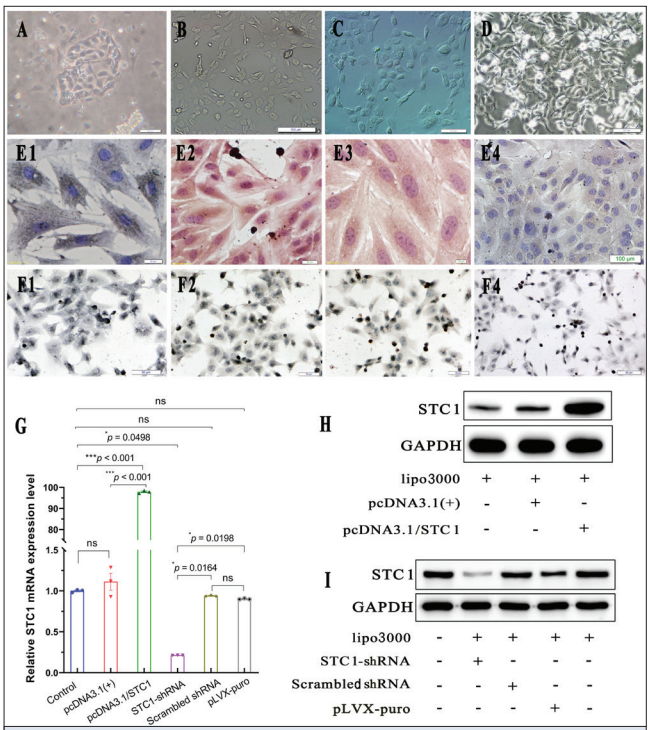

Fig 1. Characterization of morphology and immunocytochemistry in primary cultures, and expressions of STC1 in cells after transfection for 48 h. (A) Individual renal tubule epithelial cells displaying a cobblestone-like morphology, originating from adherent organoid structures in the primary cultures, scale bars=200 μm. (B) Following a series of purification steps, the cells evenly dispersed on the T25 flasks exhibiting an epithelioid cell morphology, scale bars =500μm. (C) The individual epithelial cell exhibited a dome-like, rounded morphology when observed under a phase contrast microscope, scale bars=200 μm. (D) Normal growth of MDBK cells displaying typical epithelioid cell morphology served as the positive control, scale bars=200 μm. (E1) - (E4) The cells in primary cultures stained with antibodies against PBS (as the negative control), PCK, CK18, or vimentin, respectively, scale bars=20 μm (E1), 50 μm (E2), 10 μm (E3), 100 μm (E4). (F1) - (F4) MDBK cells stained with antibodies against PBS, PCK, CK18, or vimentin, respectively, scale bars=50 μm (F1- F4). (G) The mRNA expressions of STC1 in RTECs analyzed by real-time qPCR. Each column represents a triplicate experiment (***P<0.001, **P<0.01, *P<0.05, stand for significant difference; ns stand for P>0.05, i.e., non-significant difference). (H) STC1 protein overexpression was assessed by western blotting at 48 h after transfection with pCDNA3.1(+) or pCDNA3.1/STC1. (I) Western blotting analysis to confirm the inhibition of STC1 protein expression in RTECs at 48 h post-transfection with STC1-shRNA, compared with the negative control (scrambled shRNA) and empty vector (pLVX-puro) transfected cells

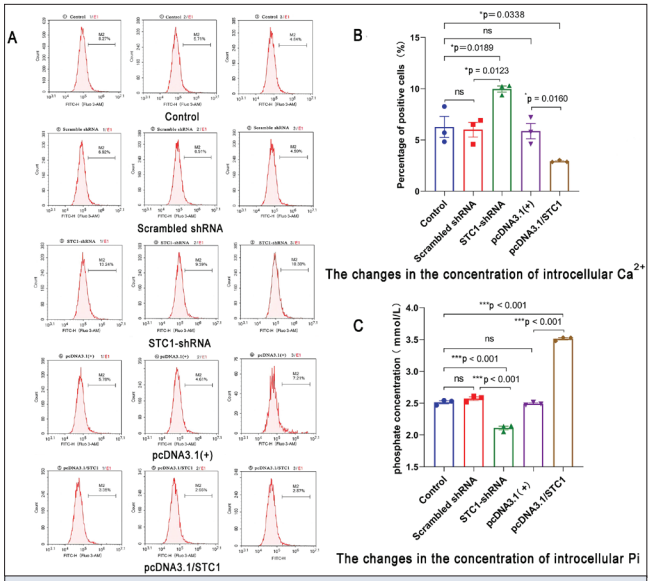

Fig 2. Changes in the intracellular free Ca^{2+} and Pi concentrations in RTECs. (A) Fluorescence histograms in the FITC-H channel from Fluo-3/AM-stained (positive for FITC-H) cells were analyzed by flow cytometry. The number of cells is displayed on the y axis and expressed as a percentage of M2, while the fluorescence intensity is shown on the x-axis. Each histogram is representative of a triplicate experiment. (B) Bar chart shows the percentages of Fluo-3/AM-positive cells, as calculated by flow cytometry. (C) Bar chart displays the intracellular Pi content in different treatment groups measured by the reduced phosphomolybdate photometric method. Note: Inhibition of STC1 by STC1-shRNA significantly increased Ca^{2+} intake (*P=0.0123) and markedly reduced Pi influx (***P<0.001), whereas STC1 overexpression via pcDNA3.1/STC1 resulted in opposite effects. Each column represents a triplicate experiment (***P<0.001, **P<0.01, *P<0.05, stand for significant difference; ns stand for P>0.05).

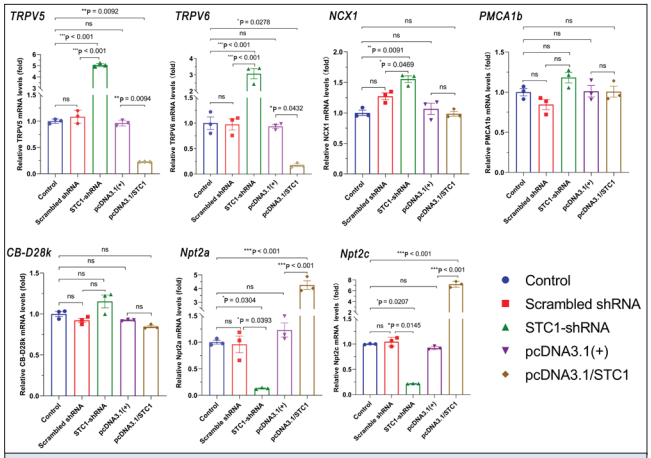

Fig 3. Bar chart showing the mRNA levels of Ca^{2+} and Pi transport proteins in RTECs cells were assessed by real-time qPCR after various treatments. Significant increases were observed in the expression levels of TRPV5, TRPV6, and NCX1 mRNA, and the levels of Npt2a and Npt2c were markedly inhibited, after 48 h transfection with STC1-shRNA. The mRNA expression levels of PMCA1b and CB-D_{28k} showed no significant changes after the inhibition of STC1. By contrast, following the overexpression of STC1 via transfection with pcDNA3.1/STC1 for 48 h, a notable decrease in the expression of TRPV5 and TRPV6 mRNA was observed, alongside a significant increase in the mRNA expression of Npt2a and Npt2c. The mRNA expression levels were corrected by *GAPDH* expression. Each column represents a triplicate experiment (***P<0.001, **P<0.01, *P<0.05, stand for significant difference; ns stand for P>0.05)

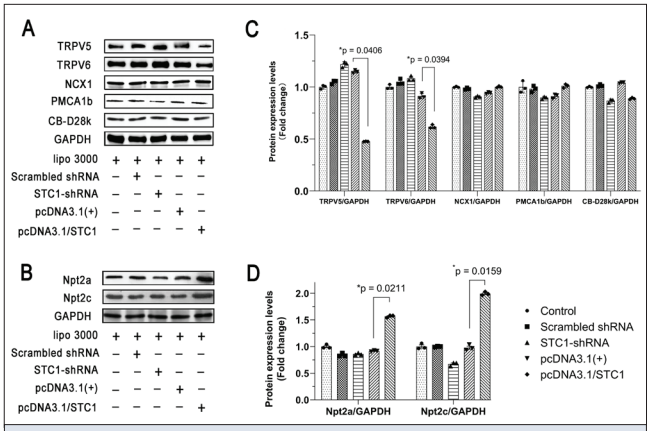

Fig 4. The protein expression levels of Ca^{2+} and Pi transport proteins in RTECs cells, as analyzed by western blotting after various treatments. (A) and (B) Specific protein bands of transcellular Ca^{2+} and Pi transport proteins. The results illustrated that the protein expression levels of TRPV5 and TRPV6 decreased significantly, and the expression levels of Npt2a and Npt2c promoted markedly, following transfection with pcDNA3.1/STC1, whereas those of NCX1, PMCA1b, and CB-D_{28k} appeared unchanged. (C) and (D) Bar charts show the densitometric analysis of the specific bands of the proteins listed in A and B, normalized to GAPDH and relative to the control group. Data are plotted as the mean ± SEM of three separate experiments, *P<0.05 *versus* the control, as determined by one-way ANOVA. The columns without marks represent a P>0.05

intracellular fluid indicates more Pi has been transported into cells, suggesting STC1 overexpression may stimulate Pi uptake by cells *(Fig. 2-C)*.

Effect of STC1 on the Expression of Ca^{2+} and Pi Transporters

After 48h transfection, real-time qPCR analysis *(Fig. 3)* showed significant increases in the mRNA expression of TRPV5 (***P<0.001), TRPV6 (***P<0.001), and NCX1 (**P=0.0091), and significant decreases in Npt2a (*P=0.0304) and Npt2c (*P=0.0207) mRNA expression, as observed in cells transfected with STC1-shRNA relative to control cells. By contrast, STC1 overexpression significantly inhibited TRPV5 (**P=0.0092) and TRPV6 (*P=0.0278) mRNA expressions, and markedly enhanced Npt2a (***P<0.001) and Npt2c (***P<0.001) mRNA expressions. However, PMCA1b, and CB-D_{28k} mRNA expressions appeared to be unaffected by the changes of STC1 expression (p>0.05).

Western blotting analysis *(Fig. 4-A,C)* further validates that STC1 overexpression significantly decreased the protein levels of TRPV5 and TRPV6, but not NCX1, PMCA1b or CB-D_{28k}. Conversely, it increased Npt2a and Npt2c levels *(Fig. 4-B,D)*. Inhibition of STC1 had no significant effect on these transporters. The densitometric analysis confirmed these findings *(Fig. 4-C,D)*.

The Interaction of STC1 with the $1,25(OH)_2D_3$/VDR Axis

After transfecting the cells with various plasmids and vectors, the results showed that STC1-shRNA transfection

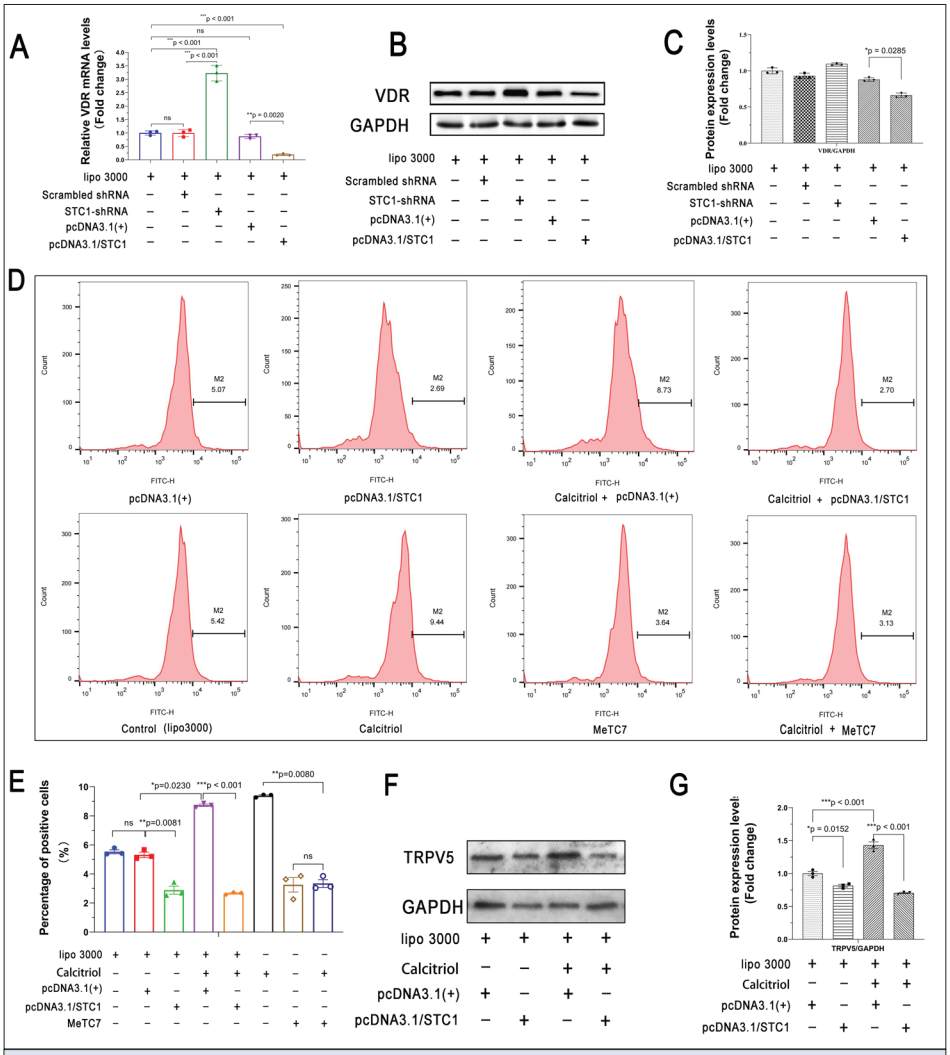

Fig 5. The interaction of STC1 with the $1,25(OH)_2D_3$/VDR axis was determined by real-time qPCR, western blotting, and flow cytometry in the RTECs. (A) Real-time qPCR analysis of VDR mRNA expressions. Transfection with STC1-shRNA for 48 h significantly enhanced VDR mRNA expression (***P<0.001), while transfection with the recombinant plasmid pcDNA3.1/STC1 notably inhibited its expression (**P=0.0020). (B) Western blotting analysis of VDR protein expression. (C) Densitometric analysis of the VDR protein bands in (B), normalized to GAPDH and expressed relative to the control group. The findings revealed that a 48-h transfection with pcDNA3.1/STC1 significantly suppressed VDR protein expression (*P=0.0285 vs. empty vector transfection group), while STC1-shRNA transfection had no significant effect on its expression (P>0.05). (D) The changes of $[Ca^{2+}]_i$) in RTECs were visualized using Fluo-3/AM staining and analyzed by flow cytometry. The cells were treated with 1% alcohol (control) or 200 nM calcitriol and then transfected with pcDNA3.1(+) or pcDNA3.1/STC1 as indicated. The results demonstrated that transfection with pcDNA3.1/STC1 significantly decreased the $[Ca^{2+}]_i$ in both untreated cells (**P=0.0081) and cells subjected to 200 nM calcitriol treatment (***P<0.001). Additionally, treatment with 250 nM MeTC7 for 12 h also significantly reduced the elevated $[Ca^{2+}]_i$ induced by 48-h calcitriol treatment (**P=0.0080). Each histogram represents the median of data from a single experiment (n=3) (F) and (G) TRPV5 expression in RTECs following 200 nM calcitriol treatment and plasmid transfection, as detected by western blotting and densitometry. The results indicated with transfection of the empty vector, 200 nM calcitriol increased TRPV5 expression following 2 days of treatment (***P<0.001). However, delivery of pcDNA3.1/STC1 to RTECs markedly weakened TRPV5 expression compared with pcDNA3.1(+) empty vector, even under 200 nM calcitriol treatment (***P<0.001)

significantly enhanced VDR mRNA expression (***P<0.001, *Fig. 5-A*). However, it did not significantly promote VDR protein expression (P>0.05, *Fig. 5-B,C*). In contrast, transfection with pcDNA3.1/STC1 remarkably suppressed both VDR mRNA (**P=0.0020, *Fig. 5-A*) and protein expression (**P=0.00285, *Fig. 5-B,C*).

To further investigate whether STC1 regulates cellular mineral absorption via $1,25(OH)_2D_3$/VDR axis, we enforced the expression of STC1 or treated cells with the VDR antagonist MeTC7 for 12 h in primary RTECs pre-treated with the VDR agonist calcitriol for 48 h. Flow cytometry results *(Fig. 5-D,E)* showed that transfection

with the control vector pcDNA3.1(+) had no influence on calcitriol-induced Ca^{2+} absorption enhancement (*P=0.0230, compared with the group transfected with the control vector only). However, overexpression of STC1, achieved via pcDNA3.1/STC1 transfection, significantly reduced the rate of detectable positive cells from an average of 8.87% (induced by 200 nM calcitriol) to ~2.67% (***P<0.001, compared with the calcitriol-treated and control vector-transfected group). In addition, after 48 h of calcitriol treatment followed by MeTC7 treatment, the detectable positive cell rate was notably reduced to an average of 3.34% from 9.39% (**P=0.0080, compared with the only calcitriol-treated group), achieving the same effect as STC1 overexpression.

To complement the above findings, the regulation of TRPV5 expression by STC1 and calcitriol was further investigated. Pre-treatment with pcDNA3.1/STC1, without calcitriol, evidently inhibited TRPV5 protein expression (*P=0.0152 vs. control vector-transfected group). Exposure of the cells to 200 nM calcitriol for 48 h followed by a transfection with the control vector up-regulated TRPV5 protein expression (***P<0.001 vs. control vector-transfected group). However, this trend was significantly reversed (***P<0.001 vs. calcitriol + pcDNA3.1/STC1 group) when cells were co-transfected with pcDNA3.1/STC1 *(Fig. 5-F, G)*.

Discussion

In dairy cattle, maintaining proper Ca^{2+}/Pi balance is vital for optimal milk production and preventing conditions like hypocalcemia, which is a common issue in post-partum cows. Elucidating the hormonal mechanisms governing Ca^{2+}/Pi regulation in dairy cows is essential for their homeostatic maintenance. Understanding these mechanisms can lead to better management practices and enhanced animal care in the dairy industry. STC1, a mineral-regulating hormone first identified in fish, is believed to play a crucial role in mammals as well.

Given the fact that numerous reports have indicated that STC1 appears to have a minor role in systemic Ca^{2+}/Pi homeostasis in mammals, it nevertheless exerts a crucial regulatory role in cellular-level Ca^{2+}/Pi transport [15]. However, the mechanism by which STC1 influences Ca^{2+}/Pi transport remains poorly understood. Our previous work demonstrated that STC1 upregulation in Caco2 cells suppressed the expression of TRPV5 and especially TRPV6 [18], and short-term exposure to low Pi and high Ca^{2+} concentration could stimulate the expression of STC-1 in RTECs, whereas its expression could be suppressed by prolonged exposure to either low or high concentrations of both Pi and Ca^{2+} (Data that has not been published in international journals). However, these data failed to reveal the interplay among STC1, channels, VDR, and Ca^{2+} absorption. In this study, we found that Ca^{2+} uptake decreased significantly after STC1 overexpression, while inhibiting STC1 had the corresponding opposite effect, suggesting that STC1 inhibits Ca^{2+} transport in bovine cells just similar to its function in intestinal tracts of swine and rats [19]. Our current research also demonstrates that STC1 influences cellular Ca^{2+}/Pi homeostasis, potentially by regulating the expression of TRPV5/6 channels, as suggested by our previous findings. These data further confirmed that ion transporters are the target of STC1, either directly or indirectly, regardless of the cell type, i.e., renal cells, intestinal cells [18], cardiomyocytes [20], zebrafish *(Danio rerio)* embryo cells [21], or gill cells [22]. Intriguingly, the downregulation of STC1 led to a notable upregulation of TRPV5/6 mRNA expression, whereas the corresponding protein levels remained unchanged. It is possible that the function of STC1 in mammalian mineral homeostasis regulation is minor or may have been compensated by alternative mechanisms or factors.

The present work found that both the mRNA and protein levels of CB-D_{28k} and PMCA1b were relatively unaffected by STC1 changes. Interestingly, the changes in STC1 expression only affect the expression of NCX1 mRNA markedly, not the protein, this was potentially associated with the fact that NCX1 serves as the primary extrusion mechanism in renal cells, where the role of PMCA1b may be of less importance [23]. Combining the previous findings [18,21], this finding further confirmed that STC1 does not influence ATP-driven Ca^{2+} efflux and Na^{+}/Ca^{2+} exchange, or cytosolic diffusion.

This study showed VDR protein levels in RTECs were markedly influenced by altering STC1 expression, specifically by STC1 overexpression. This suggests that, at least in RTECs, modulating the function of $1,25(OH)_2D_3$/VDR axis, a crucial pathway for calcium absorption [24], is a potential mechanism by which STC1 regulates the Ca^{2+} transcellular transport. Additionally, this work found that STC1 overexpression could enhance Pi absorption in RTECs, similar findings were observed in the duodenum of porcine and rats [19], as well as in the proximal tubules of fish [25]. Our findings further revealed that the enhancement of Pi absorption in RTECs was triggered by STC1 overexpression, probably achieved by upregulating the expression of Npt2a/2c, the channels mediating Pi entry.

This study supports the hypothesis that STC1 plays a conserved role in preventing Ca^{2+} transport and promoting Pi reabsorption in RTECs, specifically, were achieved by regulating Ca^{2+}/Pi influx processes mainly via impacting TRPV5/6 and Npt2a/2c expressions, respectively. STC1 appeared to have little significant effect on the Ca^{2+}/Pi intracellular diffusion and extrusion. Interestingly, the increase/inhibition in Ca^{2+}/Pi influx induced by the downregulation of STC1 seemed to be uncoupled to these channels, its downregulation possibly promotes

other mechanisms mediating Ca^{2+}/Pi absorption, which will be the focus of our future research. Given the fact that the broad distribution, diverse functions, minimal effects on body growth and development in $STC1^{(-/-)}$ mice [15,26], and the contradictory functions in multiple cancer cells [27], indicating a need for in-depth investigation into the molecular mechanisms of STC1 to determine the commonality of its effects.

This research can contribute to the development of better feeding strategies, enhanced disease prevention, and improved animal care, making it essential for both agricultural and biomedical fields. Additionally, understanding bovine Ca^{2+}/Pi regulation offers valuable insights into human health, particularly in the context of bone diseases and mineral metabolism.

Declarations

Availability of Data and Materials: The authors declare that the data and materials are available on request from the corresponding author (L. W).

Acknowledgments: We thank Liwen Bianji (Edanz) (https://www.liwenbianji.cn) for editing the language of a draft of this manuscript. We thank the Foundation of Hunan Double First-rate Discipline Construction Projects of Bioengineering and Key Laboratory of Research and Utilization of Ethnomedicinal Plant Resources of Hunan Province for providing us with a research team.

Funding Support: This research was supported by Hunan Provincial Natural Science Foundation (No. 2020JJ5450), the Scientific Research Fund of the Educational Department of Hunan Province (22B0764).

Competing Interests: The authors declare no conflicts of interest related to this work.

Declaration of Generative Artificial Intelligence (AI): The article and/or tables and figures were not written/created by AI and AI assisted technologies.

Author Contribution: Conceptualization/Resources/Supervision/Project administration/Funding acquisition, LW and XX; Formal analysis, LW; Investigation, LW, SC, XY, XW, XP, KZ, QY, YT; Methodology, LW and SC; Writing - original draft, LW, SC and XY; Writing - review & editing, LW and XX.

References

1. Hanna RM, Ahdoot RS, Kalantar-Zadeh K, Ghobry L, Kurtz I: Calcium transport in the kidney and disease processes. *Front Endocrinol,* 12:762130, 2022. DOI: 10.3389/fendo.2021.762130

2. Rohacs T, Fluck EC, De Jesús-Pérez JJ, Moiseenkova-Bell VY: What structures did, and did not, reveal about the function of the epithelial Ca^{2+} channels TRPV5 and TRPV6. *Cell Calcium,* 106:102620, 2022. DOI: 10.1016/j.ceca.2022.102620

3. Mahmoud SF, Elewa YH, Nomir AG, Rashwan AM, Noreldin AE: Calbindin has a potential spatiotemporal correlation with proliferation and apoptosis in the postnatal rat kidney. *Microsc Microanal,* 29 (5): 1705-1717, 2023. DOI: 10.1093/micmic/ozad080

4. Downie ML, Alexander RT: Molecular mechanisms altering tubular calcium reabsorption. *Pediatr Nephrol,* 37, 707-718, 2022. DOI: 10.1007/s00467-021-05049-0

5. Jennings ML: Role of transporters in regulating mammalian intracellular inorganic phosphate. *Front Pharmacol,* 14:1163442, 2023. DOI: 10.3389/fphar.2023.1163442

6. Stenhouse C, Suva LJ, Gaddy D, Wu G, Bazer FW: Phosphate, calcium, and vitamin D: key regulators of fetal and placental development in mammals. **In,** Wu G (Ed): Recent Advances in Animal Nutrition and Metabolismed., 77-107, Springer, Cham, 2021.

7. Rubio-Aliaga I, Krapf R: Phosphate intake, hyperphosphatemia, and kidney function. *Pflüg Arch Eur J Phy,* 474 (8): 935-947, 2022. DOI: 10.1007/s00424-022-02691-x

8. Song J, Qian Y, Evers M, Nielsen CM, Chen X: Cancer stem cell formation induced and regulated by extracellular ATP and stanniocalcin-1 in human lung cancer cells and tumors. *Int J Mol Sci,* 23 (23):14770, 2022. DOI: 10.3390/ijms232314770

9. Rosa RH, Jr., Xie W, Zhao M, Tsai SH, Roddy GW, Su MG, Potts LB, Hein TW, Kuo L: Intravitreal administration of stanniocalcin-1 rescues photoreceptor degeneration with reduced oxidative stress and inflammation in a porcine model of retinitis pigmentosa. *Am J Ophthalmol,* 239, 230-243, 2022. DOI: 10.1016/j.ajo.2022.03.014

10. Wu LM, Guo R, Hui L, Ye YG, Xiang JM, Wan CY, Zou M, Ma R, Sun XZ, Yang SJ, Guo DZ: Stanniocalcin-1 protects bovine intestinal epithelial cells from oxidative stress-induced damage. *J Vet Sci,* 15 (4): 475-483, 2014. DOI: 10.4142/jvs.2014.15.4.475

11. Bonfante S, Della Giustina A, Danielski LG, Denicol T, Joaquim L, Biehl E, Scopel G, de Carli RJ, Hubner M, Cardoso T, Tuon T, Generoso J, Barichello T, Terra S, Petronilho F: Stanniocalcin-1 ameliorates cerebral ischemia by decrease oxidative stress and blood brain barrier permeability. *Microvasc Res,* 128:103956, 2020. DOI: 10.1016/j.mvr.2019.103956

12. Bi SJ, Dong XY, Wang ZY, Fu SJ, Li CL, Wang ZY, Xie F, Chen XY, Xu H, Cai XJ, Zhang MX: Salvianolic acid B alleviates neurological injury by upregulating stanniocalcin 1 expression. *Ann Transl Med,* 10 (13):739, 2022. DOI: 10.21037/atm-21-4779

13. Bishop A, Cartwright JE, Whitley GS: Stanniocalcin-1 in the female reproductive system and pregnancy. *Hum Reprod Update,* 27 (6): 1098-1114, 2021. DOI: 10.1093/humupd/dmab028

14. Wu LM, Bai YY, Guo R, Yu YJ, Guo DZ: Expression of stanniocalcin-1 in the gastrointestinal tract and kidney of neonatal calves. *Pak Vet J,* 40 (1): 31-36, 2020. DOI: 10.29261/pakvetj/2019.104

15. Yeung BH, Law AY, Wong CK: Evolution and roles of stanniocalcin. *Mol Cell Endocrinol,* 349 (2): 272-280, 2012. DOI: 10.1016/j.mce.2011.11.007

16. Khazan N, Kim KK, Hansen, JN, Singh NA, Moore T, Snyder C, Pandita R, Strawderman M, Fujihara M, Takamura Y: Identification of a vitamin-D receptor antagonist, MeTC7, which inhibits the growth of xenograft and transgenic tumors *In Vivo*. *J Med Chem,* 65 (8): 6039-6055, 2022. DOI: 10.1021/acs.jmedchem.1c01878

17. Wang GQ, Lei L, Zhao XX, Zhang J, Zhou M, Nan, KJ: Calcitriol inhibits cervical cancer cell proliferation through downregulation of HCCR1 expression. *Oncol Res,* 22, 301-309, 2014. DOI: 10.3727/096504015X14424348425991

18. Xiang J, Guo R, Wan C, Wu L, Yang S, Guo D: Regulation of intestinal epithelial calcium transport proteins by stanniocalcin-1 in Caco2 cells. *Int J Mol Sci,* 17 (7):1095, 2016. DOI: 10.3390/ijms17071095

19. Madsen KL, Tavernini MM, Yachimec C, Mendrick DL, Alfonso PJ, Buergin M, Olsen HS, Antonaccio MJ, Thomson AB, Fedorak RN: Stanniocalcin: A novel protein regulating calcium and phosphate transport across mammalian intestine. *Am J Physiol-Gastr L,* 274 (1): G96-G102, 1998. DOI: 10.1152/ajpgi.1998.274.1.G96

20. Sheikh-Hamad D, Bick R, Wu GY, Christensen BM, Razeghi P, Poindexter B, Taegtmeyer H, Wamsley A, Padda R, Entman M, Nielsen S, Youker K: Stanniocalcin-1 is a naturally occurring L-channel inhibitor in cardiomyocytes: Relevance to human heart failure. *Am J Physiol-Heart C,* 285 (1): H442-H448, 2003. DOI: 10.1152/ajpheart.01071.2002

21. Tseng DY, Chou MY, Tseng YC, Hsiao CD, Huang CJ, Kaneko T, Hwang PP: Effects of stanniocalcin 1 on calcium uptake in zebrafish *(Danio rerio)* embryo. *Am J Physiol-Reg I,* 296 (3): R549-R557, 2009. DOI: 10.1152/ajpregu.90742.2008

22. Gu J, Law AY, Yeung BH, Wong CK: Characterization of stanniocalcin 1 binding and signaling in gill cells of Japanese eels. *J Mol Endocrinol,* 54 (3): 305-314, 2015. DOI: 10.1530/JME-14-0320

23. Khananshvili D: Structure-dynamic and regulatory specificities of epithelial Na^{+}/Ca^{2+} exchangers. **In,** Hamilton KL, Devor DC (Eds): Studies of Epithelial Transporters Ion Channels: Physiology in Health and Diseaseed., 325-380, Springer, Cham, 2020.

24. Jiang H, Chanpaisaeng K, Christakos S, Fleet JC: Intestinal vitamin D receptor is dispensable for maintaining adult bone mass in mice with adequate calcium intake. *Endocrinology,* 164 (5):bqad051, 2023. DOI: 10.1210/endocr/bqad051

25. Lu M, Wagner GF, Renfro JL: Stanniocalcin stimulates phosphate reabsorption by flounder renal proximal tubule in primary culture. *Am J Physiol-Reg I,* 267 (5): R1356-R1362, 1994. DOI: 10.1152/ajpregu.1994.267.5.R1356

26. Chang AC, Cha J, Koentgen F, Reddel RR: The murine stanniocalcin 1 gene is not essential for growth and development. *Mol Cell Biol,* 25 (23): 10604-10610, 2005. DOI: 10.1128/MCB.25.23.10604-10610.2005

27. Zhao F, Yang G, Feng M, Cao Z, Liu Y, Qiu J, You L, Zheng L, Zhang T, Zhao Y: Expression, function and clinical application of stanniocalcin-1 in cancer. *J Cell Mol Med,* 24 (14): 7686-7696, 2020. DOI: 10.1111/jcmm.15348